



OPEN S100A4 contributes to colorectal carcinoma aggressive behavior and to chemoradiotherapy resistance in locally advanced rectal carcinoma

Yohei Harada^{1,2}, Sayako Ikeda¹, Yuna Kawabe¹, Yasuko Oguri¹, Miki Hashimura¹, Ako Yokoi¹, Akiko Sida¹, Naomi Fukagawa^{1,2}, Misato Hayashi¹, Mototsugu Ono^{1,2,3}, Chika Kusano², Hiroyuki Takahashi³ & Makoto Saegusa¹✉

To investigate the functional role of S100A4 in advanced colorectal carcinoma (Ad-CRC) and locally advanced rectal carcinoma (LAd-RC) receiving neoadjuvant chemoradiotherapy (NCRT). We analyzed histopathological and immunohistochemical sections from 150 patients with Ad-CRC and 177 LAd-RC patients treated with NCRT. S100A4 knockout (KO) HCT116 cells were also used. S100A4 expression was absent in normal mucosa but increased progressively from colorectal adenoma to carcinoma, suggesting that S100A4 regulation is an early event in colorectal carcinogenesis. In Ad-CRC, high S100A4 expression correlated with high tumor budding and nuclear β -catenin, deep invasion, lymphovascular involvement, and unfavorable prognosis. In NCRT-treated LAd-RC, high S100A4 expression was associated with poor treatment response and short progression-free survival. S100A4 KO decreased the proliferation of HCT116 cells through activation of the p53/p21^{waf1} axis, and sensitized cells to adriamycin-induced apoptosis. Levels of the apoptotic marker, cleaved poly (ADP-ribose) polymerase 1, were significantly higher in samples with low S100A4 and wild type p53. Finally, we observed a direct interaction between S100A4 and p53. In conclusion, S100A4 expression engenders aggressive behavior in Ad-CRC through association with β -catenin-driven tumor buddings. S100A4 exerts anti-apoptotic and proliferative effects via inhibition of p53 in LAd-RC patients receiving NCRT, which leads to chemoradioresistance and poor prognosis.

Keywords S100A4, p53, Apoptosis, Colorectal carcinoma, Neoadjuvant chemoradiotherapy

Colorectal carcinoma (CRC) is one of the most common malignancies worldwide and a major cause of carcinoma death¹. Approximately 70% of CRC cases are sporadic and caused by environmental factors, with genetic predisposition and familial mutations accounting for the remaining 30%^{2,3}. The incidence of CRC in Asia (especially in Japan, China, Korea, and Taiwan) is rising steadily, with a two- to four-fold increase over the last few decades⁴.

Five-year overall survival for patients with stage I CRC is approximately 90%; this decreases to about 10% for stage IV patients⁵. The stage IV patient group contains individuals with advanced CRC, and locally advanced rectal carcinoma (Ad-CRC and LAd-RC hereafter). Prior to total mesorectal excision in these patients, neoadjuvant chemoradiotherapy (NCRT) is performed to induce downstaging, downsizing, and significant changes in histological characteristics^{6,7}. Although this increases the response rate to systemic NCRT to 50%, nearly all patients with LAd-RC subsequently develop resistance^{8–10}. Understanding the molecular mechanisms that drive NCRT resistance may therefore elucidate novel therapeutic strategies to prolong patient life.

S100A4 belongs to the S100 family and is a calcium-binding protein with two EF-hand domains^{11–13}. The S100 proteins do not have enzymatic activity and instead exert their biological activities through interaction with target proteins^{11–13}. In particular, S100A4 contributes to tumor progression, through modulation of cell motility, adhesion, proliferation, and invasion. Although aberrant S100A4 expression is a useful biomarker

¹Department of Pathology, Kitasato University School of Medicine, 1-15-1 Kitasato, Minami-ku, Sagami-hara 252-0374, Kanagawa, Japan. ²Department of Gastroenterology, Kitasato University School of Medicine, 1-15-1 Kitasato, Minami-ku, Sagami-hara 252-0374, Kanagawa, Japan. ³Department of Pathology, Kitasato University School of Allied Health Science, 1-15-1 Kitasato, Minami-ku, Sagami-hara 252-0374, Kanagawa, Japan. ✉email: msaegusa@med.kitasato-u.ac.jp

of chemo- or radio-resistance in several human malignancies^{14,15}, the molecular mechanisms underpinning S100A4-dependent resistance to NCRT remain unclear.

To address this gap in knowledge, we profiled the expression of S100A4 during Ad-CRC progression, and examined its relationship with β -catenin, a known S100A4 regulator¹⁶. We also examined the role of S100A4 in NCRT-treated LAd-RC and CRC cell lines using CRISPR knockout (KO) technology.

Methods

Clinical cases

We evaluated pathological specimens of 150 Ad-CRC cases without NCRT treatment, surgically resected between 2009 and 2021, at Kitasato University Hospital, according to the criteria of the Japanese Classification of Colorectal, Appendiceal, and Anal Carcinoma and the TMN classification^{17,18}. We also selected 179 LAd-RC patients, with clinical T3 or T4, N0 to N2, or M0 tumors, who underwent NCRT¹⁹, followed by total mesorectal excision at Kitasato University Hospital between 2006 and 2021. Of these, 55 also received post-surgical adjuvant chemotherapy (capecitabine and oxaliplatin regimen). The demographic and clinicopathological data in Ad-CRC and NCRT-treated LAd-RC cases are summarized in Supplementary Table S1. Pretreatment-biopsied samples from 106 NCRT-treated LAd-RC patients were also investigated. In addition, 20 samples of normal colorectal epithelium adjacent to the tumors, low-grade adenoma, high-grade adenoma, carcinoma in adenoma, and non-invasive CRC, respectively, were also examined. This study was approved by the Kitasato University Medical Ethics Committee (B19-155).

Evaluation of histopathological findings

Tumor budding (BD)²⁰ and the BD score was evaluated according to the criteria of the Japanese Classification of Colorectal, Appendiceal, and Anal Carcinoma¹⁷. Ad-CRC lesions were subcategorized into three groups based on the depth of tumor invasion as follows: mucosal (m), submucosal (sm), and muscularis propria/subserosal (mp/ss) layers. NCRT-treated LAd-RC cases were also subclassified into three groups on the basis of the therapeutic efficacy (TE) of NCRT, as follows: grade (G) 1, mild efficacy; G2, moderate; and G3, no tumor elements, according to the criteria of the Japanese Classification of Colorectal, Appendiceal, and Anal Carcinoma¹⁷.

Immunohistochemistry (IHC)

IHC was performed using a combination of microwave-oven heating and immuno-enzyme polymer (Nichirei Bioscience Inc, Tokyo, Japan) and the evaluation of S100A4 score and nuclear β -catenin and Ki-67 immunopositive labeling indices (LIs) was performed as described previously²¹. The S100A4 scores and nuclear β -catenin LIs were subdivided into two categories based on the mean – standard deviation (SD), mean, or median values, as cutoff (Supplementary Figure S1). p53 immunopositivity was subdivided into mutant (mt, 0% or 60–100%) and wild type (wt, 1–59%) classes²². The cleaved PARP1 IHC score was derived from counting cells in five randomly selected high-power fields (HPFs).

Cell line and plasmids

An S100A4 KO CRC cell line was generated using HCT-116 (ATCC, Manassas, VA, USA). Briefly, the guide RNA sequence (gRNA: 5'-CCACAAGTACTCGGGCAAAG-3') was designed using CRISPRdirect (<https://crispr.dbcls.jp>) and cloned into pSpCas9n(BB)-2 A-Puro (PX459) V2.0 (Addgene #62988) to establish the S100A4 KO cell line as described previously²¹. We also used the following plasmids: pcDNA- β -catenin Δ ^{S45}, pCI-p300, pGL3B(-1976/+1012) S100A4-luc, and pCMVp53wt as described previously^{23,24}.

Antibodies and reagents

Antibodies are listed in Supplementary Table S2. Adriamycin (ADR) was obtained from Sigma-Aldrich Chemicals (St. Louis, MO, USA).

Western blot and co-immunoprecipitation (co-IP) assays

Isolation of total cellular proteins and western blot and co-IP assays were carried out as described previously^{21–25}. The signals were analyzed using ImageJ software version 1.41 (NIH, Bethesda, MD, USA; <http://imagej.nih.gov/ij>) as described previously²⁵. The reconstructed images of all blots with membrane edges visible are accessible in the Supplementary Materials, because some of the original full-length blots were cut prior to hybridization with antibodies.

Flow cytometry

Cell cycle analysis was performed using a BD FACS Calibur instrument (BD Biosciences, Franklin Lakes, NJ, USA) and CellQuest Pro software v3.3 (BD Biosciences) as described previously^{21,25}.

Proximity ligation assay (PLA)

Mouse β -catenin or mouse p53 were used alone (negative controls) or in combination with rabbit S100A4 antibody. The slides were treated using the Duolink Detection kit with PLA PLUS and MINUS probes for mouse and rabbit antibodies, respectively (Olink Bioscience, Uppsala, Sweden). The average number of intranuclear and intracytoplasmic PLA signals was expressed as signals per cell as described previously²⁶.

Cell Counting Kit-8 assay

Cell viability after ADR treatment was evaluated using the Cell Counting Kit-8 (CCK-8; Dojindo Lab, Kumamoto, Japan), according to the manufacturer's instructions.

Apoptotic index

The number of apoptotic cells identified in HE-stained sections was calculated by counting the mean number of apoptotic figures per field as described previously²⁷.

Transfection and luciferase assay

Transfection was carried out using LipofectAMINE PLUS (Invitrogen, Carlsbad, CA, USA) and luciferase activity was assayed 24 h after transfection using the Dual-luciferase reporter assay system (Promega) as described previously^{24,25}.

Statistical analysis

Comparative data were analyzed using the Mann-Whitney *U*-test and Chi-square test, as appropriate. Overall survival (OS), progression-free survival (PFS), and recurrence-free survival (RFS) were also examined from the onset of treatment until relapse (recurrence), disease progression, or last follow-up evaluation. Univariate and multivariate analyses were performed using the Cox proportional hazards regression model. The cutoff for statistical significance was set as $P < 0.05$.

Results

Upregulation of S100A4 in development and progression of CRC

Nuclear/cytoplasmic S100A4 immunoreactivity was observed in colorectal tumors but not normal mucosal lesions (Fig. 1A), with a significant stepwise increase in expression from adenomas to non-invasive CRC (Fig. 1B).

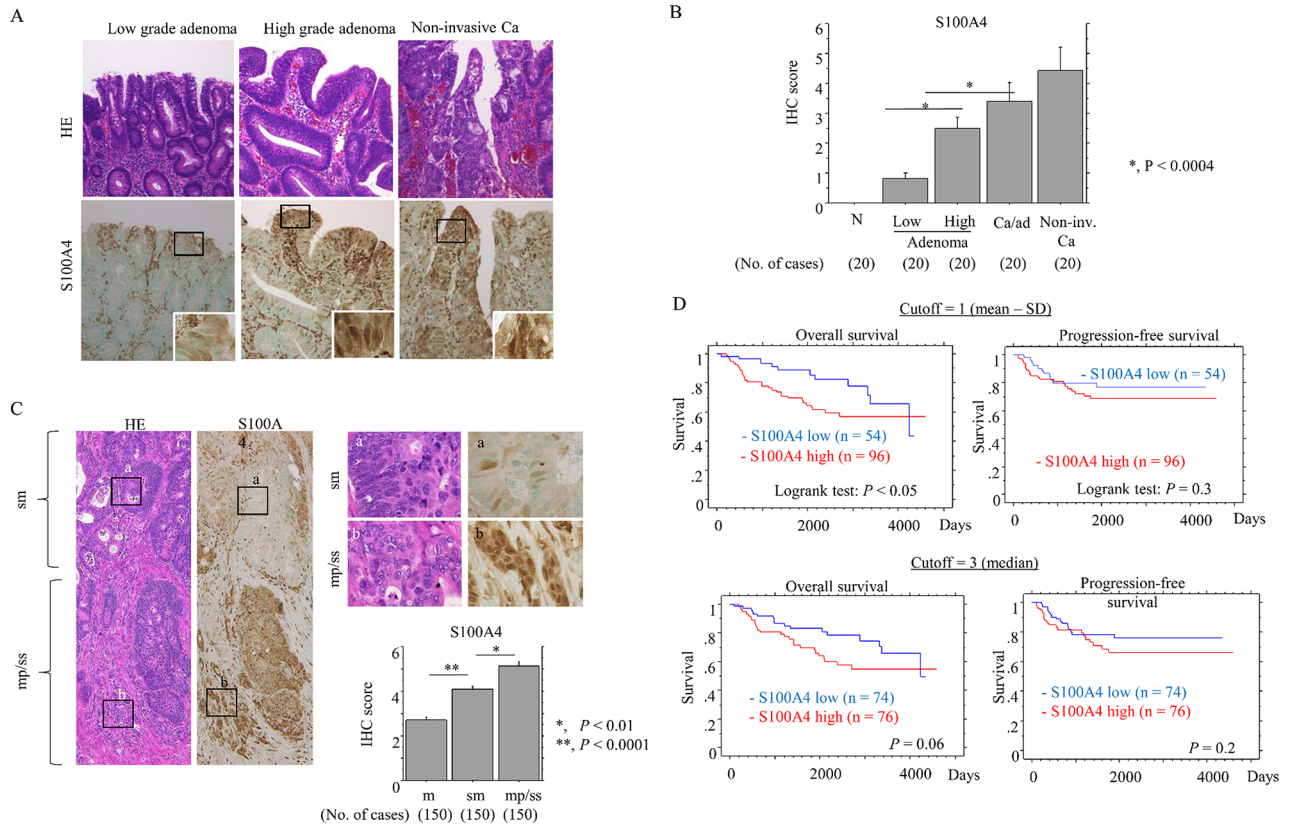


Fig. 1. Progressive upregulation of S100A4 in the colorectal adenoma-carcinoma transition and Ad-CRC. **(A)** Staining with HE and IHC for S100A4 in low- and high-grade colorectal adenoma and non-invasive CRC (Ca). Closed boxes in the lower panels are magnified in insets. Original magnification, x200 and x400 (insets). **(B)** IHC scores for S100A4 in samples from normal (N), low- and high-grade adenomas, carcinoma in adenoma (Ca/ad), and non-invasive CRC (Non-inv. Ca). The scores are shown as mean \pm SD. Statistical analyses were carried out using the Mann-Whitney *U*-test. **(C)** Left and right-upper: staining with HE and IHC for S100A4 in Ad-CRC. The closed boxes in left panels are magnified in the upper-right panels. Original magnification, x40 (left panels) and x400 (upper-right panels). Lower-right: IHC scores for S100A4 between mucosal (m), submucosal (sm), and muscularis propria (mp)/subserosal (ss) Ad-CRC lesions. The scores are shown as mean \pm SD. Statistical analyses were carried out using the Mann-Whitney *U*-test. **(D)** OS (left) and PFS (right) relative to S100A4 (low versus high expression) based on the mean - SD (upper) and median values (lower) as cutoffs in Ad-CRC. n, number of cases.

S100A4 scores were significantly higher in Ad-CRC tumors localized at mp/ss lesions (including the tumor invasive front) as compared to m and sm lesions (Fig. 1C). High S100A4 expression was significantly associated with highly invasive tumors, high tumor budding, lymphovascular invasion (Table 1), and the poorest OS (Fig. 1D). Comparison of univariate and multivariate Cox analyses revealed that S100A was a significant (but not independent) prognostic indicator for OS (Table 2).

High nuclear β -catenin was also significantly associated with the tumor invasive front but did not correlate with prognosis in Ad-CRC (Supplementary Figure S2). The PLA assay, which can be used to quantify protein-

	n	S100A4 IHC score		P-value
		High (≥ 1)	Low (< 1)	
		n (%)	n (%)	
Gender				
Male	78	53 (67.9)	25 (32.1)	0.2
Female	72	43 (59.7)	29 (40.3)	
Age				
≤ 68 year	74	45 (60.8)	29 (39.2)	0.4
≥ 69 year	76	51 (67.1)	25 (32.9)	
Tumor location				
Right colon	48	30 (62.5)	18 (37.5)	0.7
Left colon	102	66 (64.7)	36 (35.3)	
Macroscopic findings				
Depression	135	89 (65.9)	46 (34.1)	0.1
Elevation	15	7 (46.7)	8 (53.3)	
Histology				
Tub	134	85 (63.4)	49 (36.6)	0.6
Muc,por,sig	16	11 (68.8)	5 (31.2)	
Tumor size				
≤ 4.2 cm	84	51 (60.7)	33 (39.3)	0.3
≥ 4.3 cm	66	45 (68.2)	21 (31.8)	
Depth				
Less than MP	39	19 (48.7)	20 (51.3)	0.02
More than SS	111	77 (69.4)	34 (30.6)	
Tumor budding				
BD1	82	43 (52.4)	39 (47.6)	0.001
BD2/3	68	53 (77.9)	15 (22.1)	
Ly invasion				
Positive	85	61 (71.8)	24 (28.2)	0.02
Negative	65	35 (53.8)	30 (46.2)	
V invasion				
Positive	122	83 (68.0)	39 (32.0)	0.03
Negative	28	13 (46.4)	15 (53.6)	
LN metastasis				
Positive	62	41 (66.1)	21 (33.9)	0.6
Negative	88	55 (62.5)	33 (37.5)	
Distant metastasis				
Positive	16	13 (81.3)	3 (18.7)	0.1
Negative	134	83 (61.9)	51 (38.1)	
Pathological stage				
I/II	83	50 (60.2)	33 (39.8)	0.2
III/IV	67	46 (68.7)	21 (31.3)	

Table 1. Relationship between S100A4 expression and clinicopathological factors in advanced colorectal carcinoma cases without NCRT. tub, tubular; muc, mucinous; por, poorly; sig, signet; MP, muscularis propria; SS, subserosal; Ly, lymph vessel; V, venous vesse; LN, lymph node. Pathological stage refers to the criteria of the Japanese Classification of Colorectal, Appendiceal, and Anal carcinoma.

Variables	Univariate analysis				Multivariate analysis		
	Cut-off	Logrank c2	P-value	unfavorable factor	Hazard ratio	95% CI	P-value
Overall survival							
Gender	Male/female	0.11	0.7				
Age (years)	68/69	7.31	0.006	> 69	2.169	1.12–4.21	0.02
Location	R/L	1.11	0.2				
Macroscopic type	Depression/uplift	1.77	0.1				
Histology	Tub/others	1.43	0.2				
Tumor size	4.2/4.3	1.99	0.1				
Depth	MP/SS,SE	10.29	0.001	SS,SE	0.357	0.12–1.05	0.06
Lymphatic invasion	(-)/(+)	1.33	0.2				
Venous invasion	(-)/(+)	1.16	0.2				
LN metastasis	(-)/(+)	7.67	0.005	+	0.725	0.17–3.07	0.6
Distant metastasis	(-)/(+)	30.02	< 0.0001	+	0.25	0.11–0.61	0.002
Pathological stage	I, II/III, IV	12.47	0.0004	III, IV	1.1	0.21–5.82	0.9
BD score	1/2,3	15.26	< 0.0001	2,3	2.36	1.18–4.72	0.01
S100A4 expression	Low/High	3.92	0.04	High	1.345	0.63–2.82	0.4
Progression-free survival							
Gender	Male/female	0.21	0.6				
Age (years)	68/69	3.37	0.06				
Location	R/L	0.02	0.8				
Macroscopic type	Depression/uplift	–	–				
Histology	Tub/others	0.26	0.6				
Tumor size	4.2/4.3	0.08	0.7				
Depth	MP/SS,SE	8.81	0.003	SS,SE	0.355	0.11–1.22	0.1
Lymphatic invasion	(-)/(+)	0.51	0.4				
Venous invasion	(-)/(+)	6.09	0.01	+	0.196	0.02–1.46	0.1
LN metastasis	(-)/(+)	10.52	0.001	+	0.539	0.05–5.01	0.5
Distant metastasis	(-)/(+)	4.82	0.02	+	0.709	0.24–2.03	0.5
Pathological stage	I, II/III, IV	11.59	0.0007	III, IV	0.94	0.08–10.23	0.9
BD score	1/2,3	5.33	0.02	2,3	1.615	0.78–3.33	0.1
S100A4 expression	Low/High	1.05	0.3				

Table 2. Univariate and multivariate analyses for overall survival and progression-free survival in advanced colorectal carcinoma without NCRT treatment. LN, lymph node; BD, tumor budding; MP, muscularis propria; SS, subserosal, SE, serosa exposure; (-), negative; (+), positive. Macroscopic type and pathological stage refer to the criteria of the Japanese Classification of Colorectal, Appendiceal, and Anal carcinoma.

protein interactions in tissue Sect²⁸, revealed significantly more nuclear S100A4/ β -catenin foci in the tumor invasive front, including at site of tumor budding (Supplementary Figure S3A); this contrasted with a lack of signal following co-IP experiments (Supplementary Figure S3B). In addition, the *S100A4* promoter was significantly activated by co-transfection of β -catenin and p300 (Supplementary Figure S3C).

Relationship between S100A4 and NCRT resistance in LAd-RC

The results of S100A4 and Ki-67 immunoreactivity in resected LAd-RCs after NCRT are shown in Fig. 2A. The S100A4 scores and Ki-67 LIs were significantly higher in patients who responded poorly to NCRT (TE: G1) compared to those patients with TE: G2. High S100A4 expression was associated with the shortest PFS in NCRT-treated LAd-RC patients (Fig. 2B). Patients with R1 resection were associated with a more unfavorable OS and PFS compared to patients with R0 resection (Supplementary Figure S4A). High S100A4 expression was significantly associated with the poorest RFS but not OS in R0 resection, whereas such associations were not evident in R1 resection (Supplementary Figure S4B). Moreover, patients receiving post-surgical adjuvant chemotherapy also had poorer OS and PFS compared to those who did not receive chemotherapy (Supplementary S5A). In addition, high S100A4 expression was associated with poor PFS in patients without post-surgical adjuvant chemotherapy (Supplementary Figure S5B).

Comparison of univariate and multivariate Cox analyses revealed that S100A4 expression was a significant (but not independent) prognostic indicator of PFS (Table 3). Nuclear β -catenin status was not a prognostic indicator of PFS (Supplementary Figure S6). In addition, S100A4 scores in pretreatment-biopsied samples from LAd-RC patients did not correlate with TE grade in surgical specimens (Supplementary Figure S7).

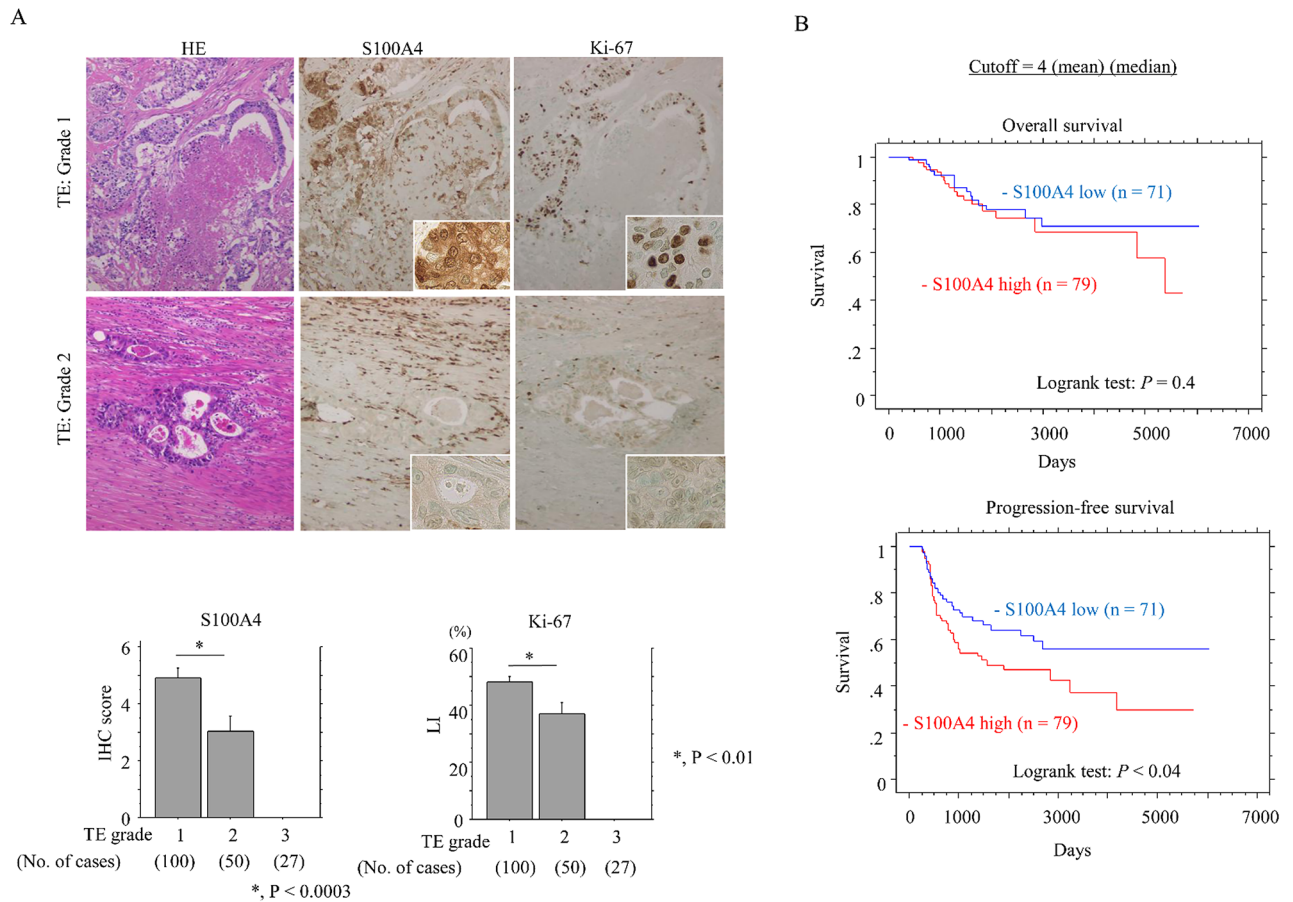


Fig. 2. Relationship between S100A4 expression and chemoradioresistance in NCRT-treated LAd-RC. **(A)** Upper: staining with HE and IHC for the indicated proteins in LAd-RC samples that respond poorly to NCRT (TE: Grade 1) (upper panels) or moderately (TE: Grade 2) (lower panels). The closed boxes in IHC panels are magnified in insets. Original magnification, x200 and x400 (insets). Lower: S100A4 IHC scores and Ki-67 LIs in samples from NCRT-treated LAd-RC patients. The scores and LIs are shown as mean \pm SD. Statistical analyses were carried out using the Mann-Whitney U-test. **(B)** OS (upper) and PFS (lower) relative to S100A4 (low versus high expression) based on the mean and median values as cutoff in LAd-RC receiving NCRT. n, number of cases.

Knockout of S100A4 decreases proliferation and sensitizes to apoptosis

To examine the functional role of S100A4 in NCRT resistance in LAd-RC, we generated two independent S100A4 KO HCT116 cell line clones (KO#3 and KO#4). In response to ADR treatment, S100A4 KO significantly decreased cell viability when compared to parental cells (Fig. 3A). Consistent with this, we observed increased apoptosis (Fig. 3B) and sub-G1 fraction (Fig. 3C), as well as increased expression of cleaved caspase-3, cleaved poly (ADP-ribose) polymerase-1 (PARP1), and BCL-2 (Fig. 3D and Supplementary Figure S8); an exception was the lack of increased cleaved PARP1 in S100A4 KO#4 cells.

S100A4-KO cells also proliferated more slowly than parental cells; consistent with this, there were proportionally less cells in S phase (Fig. 4A). We next examined the impact of S100A4 loss on several cell cycle-related markers. First, S100A4 KO cells were rendered quiescent by serum starvation. We then added back serum to trigger cell cycle entry, and took samples for western blot at 7 and 24 h post-serum stimulation. Levels of cyclin A2 and cyclin B1 were lower in S100A4 KO cells when compared to parental cells, whereas p21^{waf1} expression was higher (Fig. 4B and Supplementary Figure S9).

Relationship between S100A4 expression and p53-dependent apoptosis

Since p53 interacts directly with S100A4^{28–31}, we examined whether there was a functional interaction between these two proteins in NCRT-treated LAd-RC. A PLA assay revealed distinct nuclear dots containing S100A4 and p53 in LAd-RC (Fig. 5A). This indication that they interact in LAd-RC was supported by the results of co-IP assay (Fig. 5B and Supplementary Figure S10A). There was no significant difference in p53 protein stability between S100A4 KO and parental cells (Fig. 5C and Supplementary Figure S10B). In addition, S100A4 promoter activity was significantly repressed by transfection of p53 (Supplementary Figure S11). Finally, the percentage of cleaved PARP1-positive cells was significantly higher in S100A4-low as compared to S100A4-high NCRT-

Variables	Univariate analysis				Multivariate analysis		
	Cut-off	Logrank c2	P-value	unfavorable factor	Hazard ratio	95% CI	P-value
Overall survival							
Gender	Male/female	4.95	0.02	male	0.35	0.11–1.092	0.07
Age (years)	63/64	0.96	0.3				
Macroscopic type	Type1-4/type5	0.57	0.4				
Histology type	Tub/others	1.89	0.1				
Tumor size	3.1/3.2	15.95	<0.0001	> 3.2	2.71	1.03–7.15	0.04
Depth	mp/ss,se	6.11	0.01	SS,SE	0.75	0.20–2.80	0.6
Lymphatic invasion	(-)/(+)	5.32	0.02	+	0.67	0.29–1.54	0.3
Venous invasion	(-)/(+)	4.21	0.04	+	0.62	0.23–1.67	0.3
LN metastasis	(-)/(+)	19.95	<0.0001	+	0.38	0.15–0.97	0.04
Distant metastasis	(-)/(+)	16.23	<0.0001	+	0.28	0.12–0.67	0.004
Residual tumor	R0/R1	10.98	0.0009	R1	0.48	0.19–1.24	0.1
Post-surgical chemotherapy	(-)/(+)	11.593	0.0004	+	0.77	0.33–1.80	0.5
Treatment Effect	Grade 1/Grade 2	3.22	0.07				
S100A4 expression	Low/High	0.55	0.4				
Progression-free survival							
Gender	Male/female	1.03	0.3				
Age (years)	63/64	2	0.2				
Macroscopic type	Type1-4/5	4.31	0.03	type1-4	0.87	0.52–1.47	0.6
Histology type	Tub/others	7.41	0.006	others	0.62	0.26–1.46	0.2
Tumor size	3.1/3.2	14.21	0.0002	> 3.2	1.6	0.85–3.01	0.1
Depth	mp/ss,se	8.51	0.003	SS,SE	0.65	0.24–1.76	0.3
Lymphatic invasion	(-)/(+)	5.56	0.01	+	0.94	0.52–1.68	0.8
Venous invasion	(-)/(+)	1.58	0.2				
LN metastasis	(-)/(+)	20.86	<0.0001	+	0.71	0.36–1.37	0.3
Distant metastasis	(-)/(+)	5.28	0.02	+	0.68	0.34–1.36	0.2
Residual tumor	R0/R1	29.52	<0.0001	R1	0.68	0.34–1.33	0.2
Post-surgical chemotherapy	(-)/(+)	30.58	<0.0001	+	0.51	0.28–0.941	0.03
Pathological stage	I, II/III, IV	11.55	0.0007	II, III, IV	2.38	0.69–8.14	0.1
Clinical stage	I, II/III, IV	5.65	0.01	III, IV	0.99	0.52–1.90	0.9
Treatment Effect	Grade 1/Grade 2	3.61	0.05				
S100A4 expression	Low/High	4.25	0.03	High	1.62	0.93–2.80	0.08

Table 3. Univariate and multivariate analyses for overall survival and progression-free survival in NCRT-treated locally advanced colorectal carcinoma. NCRT, neoadjuvant chemoradiotherapy; LN, lymph node; BD, tumor budding; mp, muscularis propria; ss, subserosal, se, serosa exposure; (-), negative; (+), positive. R0, no residual tumor; R1, residual tumor. Pathological stage refers to the criteria of the Japanese Classification of Colorectal, Appendiceal, and Anal carcinoma.

treated-LAd-RC cases (Fig. 6A), with the highest percentage being found in the “S100A4-low, p53wt” group (Fig. 6B).

Discussion

In this report, we clearly show that S100A4 expression progressively increases as cells transition from normal tissue to adenoma and then to non-invasive CRC. Moreover, loss of S100A4 robustly reduces molecular markers of the cell cycle, which ultimately leads to decreased proliferation. These observations are consistent with early reports that S100A4 is highly expressed in both growth factor-stimulated normal cells^{32,33}, and in metastatic tumor cell lines³⁴. It has been suggested that S100A4 overexpression is an early event during colorectal carcinogenesis, and that it enhances the malignant potential of early tumor cells^{35,36}.

Tumor budding at the invasive front is a reliable histopathological marker for estimating CRC aggressiveness^{37,38}. We found that high S100A4 expression was also significantly associated with tumor budding in Ad-CRC. Although nuclear foci containing S100A4 and β -catenin (which is also associated with tumor budding²⁵) were more abundant at the tumor invasive front, these proteins did not co-immunoprecipitate. Given that the *S100A4* promoter was activated by a β -catenin/p300 complex, we suggest that S100A4 may indirectly cooperate to establish and maintain β -catenin-dependent tumor budding in Ad-CRC. Further studies, including monitoring the levels of β -catenin mRNA or protein after manipulation of S100A4 levels, are required to address this hypothesis.

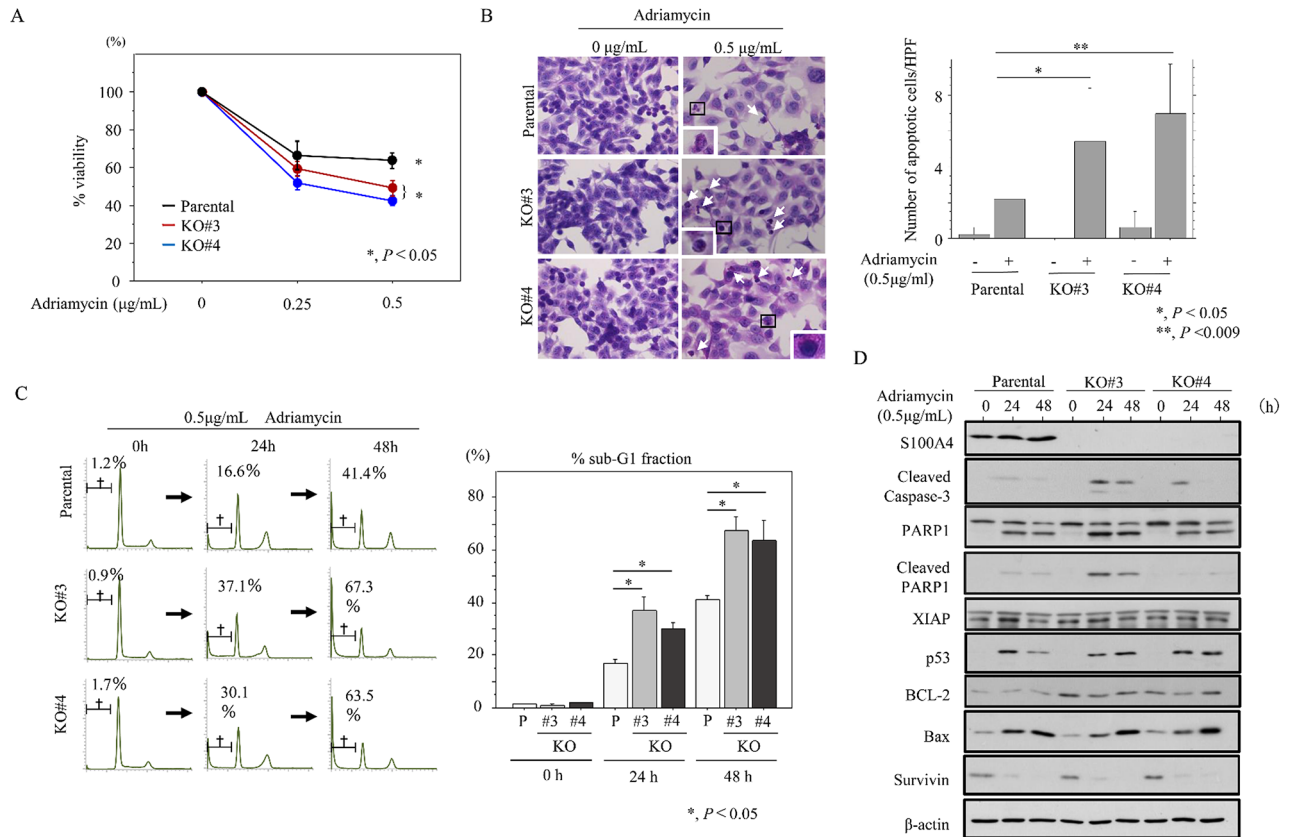


Fig. 3. Changes in susceptibility to apoptosis following S100A4 knockout in CRC cells. **(A)** Treatment of S100A4 KO and parental cells with the indicated doses of ADR for 24 h. Viability in the absence of ADR treatment is set as 100%. The experiments were performed in triplicate. **(B)** Left: after 0.5 µg/mL ADR treatment, cells undergoing apoptosis in the S100A4 KO and parental lines are indicated with arrows. The closed boxes in right panels are magnified in the insets. Original magnification, x200 and x400 (insets). Right: number of apoptotic cells is shown as mean ± SD. Statistical analyses were carried out using the Mann-Whitney U-test. **(C)** Left: flow cytometric cell cycle analysis for S100A4 KO and parental cells after 0.5 µg/mL ADR treatment for the time shown. Daggers indicate sub-G1 fractions. Right: the percentages of cell undergoing apoptosis (sub-G1) were calculated. The experiments were performed in triplicate. **(D)** Western blot analysis for the indicated proteins in total lysates from S100A4 KO and parental cells treated with 0.5 µg/mL ADR treatment for the times shown. The experiments were performed in triplicate.

The impact of S100A4 levels on the response to chemotherapy appears context-dependent. For example, a CRC cell line resistant to doxorubicin had moderate S100A4 expression³⁹, whereas sensitivity to 5-fluorouracil was independent of S100A4 in other CRC cell lines⁴⁰. In our current study, we found that high S100A4 expression was associated with chemoradioresistance and poor prognosis in NCRT-treated LAd-RC. A similar association with S100A4 expression was also evident in patients with R0 resection and without post-surgical adjuvant chemotherapy. Together, these observations indicate an important role of S100A4 as a prognostic factor in NCRT-treated LAd-RC. By contrast, the lack of association between S100A4 levels in pretreatment-biopsied samples and NCRT efficacy in the corresponding resected RC samples may be due to the heterogeneous expression of S100A4 in LAd-RC tissues.

In tissues from LAd-RC patients who received NCRT, we found that low S100A4 expression was significantly associated with a high score for cleaved PARP1, which is a major product of caspase-3 activity in vivo⁴¹. Moreover, S100A4 KO enhanced susceptibility to ADR-induced apoptosis, suggesting that S100A4 acts as a pro-survival factor by suppressing the apoptotic pathway in response to NCRT in LAd-RC. Similar findings have also been observed in pancreatic ductal adenocarcinoma and osteosarcoma^{42,43}.

Finally, we found that p53 wild type cells with little or no S100A4 were much more sensitive to chemoradiotherapy-induced apoptosis than their p53 mutant counterparts. Given that S100A4 directly interacted with p53 in both LAd-RC tissue and CRC cell line, we suggest that S100A4 effectively blocks p53 activation and DNA binding, thereby facilitating cell survival and NCRT resistance in LAd-RC. A corollary is that a negative feedback loop may also operate, in which p53 represses the *S100A4* promoter.

There were several limitations to this study. For example, we were unable to analyze protein expressions in TE: G3 cases, because of the complete tumor regression elicited by NCRT treatment. Additionally, our study was retrospective and based on a relatively small number of Ad-CRC and NCRT-treated LAd-RC cases from a single department. Although we were able to extract more -detailed patient data than other studies (including clinical

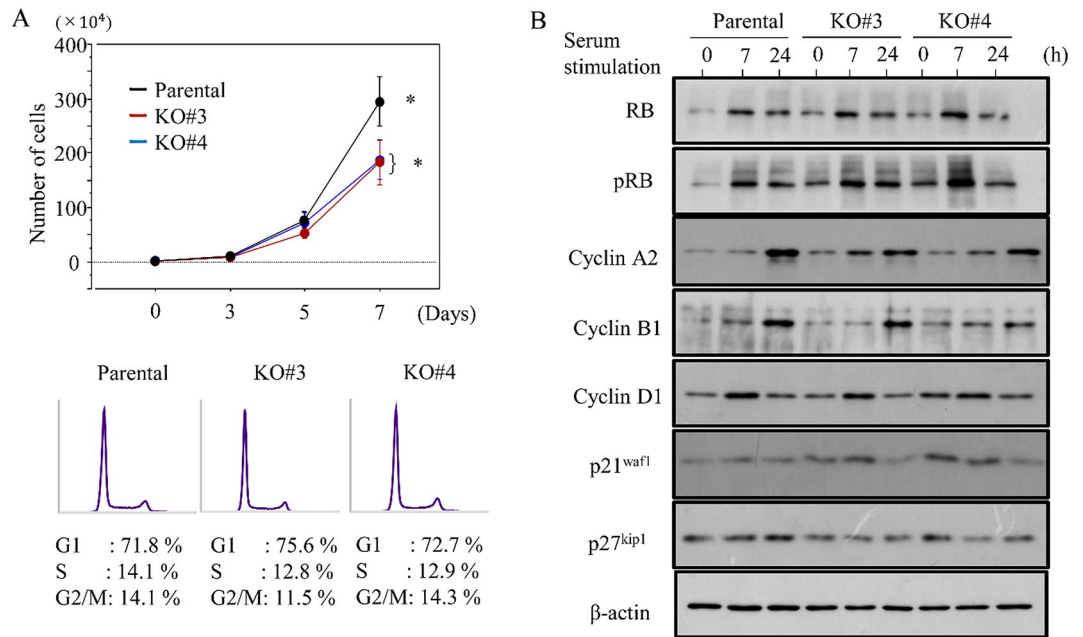


Fig. 4. Changes in proliferation following S100A4 knockout in CRC cells. **(A)** Upper: S100A4 KO and parental cells were seeded at low density. Cell numbers are presented as mean ± SD. P0, P3, P5, and P7 are 0, 3, 5, and 7 days after seeding, respectively. The experiments were performed in triplicate. Lower: flow cytometry analysis of S100A4 KO and parental cells 3 days after seeding (P3). **(B)** Western blot analysis for the indicated proteins in total lysates from S100A4 KO and parental cells following re-stimulation of serum-starved (24 h) cells with 10% serum for the indicated times.

variables, pathology results, and treatment outcomes), we acknowledge that larger-scale multicenter studies will be required in the further to fully evaluate the prognosis of Ad-CRC and NCRT-treated LAd-RC patients.

Conclusion

Our results show that elevated S100A4 expression engenders aggressive behavior in Ad-CRC through indirect modulation of nuclear β-catenin-mediated tumor budding. S100A4 also inhibits apoptosis and favors proliferation, at least partly due to attenuation of p53; this is in turn associated with chemoradioresistance and poor prognosis in LAd-RC (Fig. 7). Further studies could establish a new therapy for Ad-CRC and NCRT-treated LAd-RC using S100A4-targeted agents.

Table 2 Univariate and multivariate analyses for overall survival and progression-free survival in advanced colorectal carcinoma without NCRT treatment.

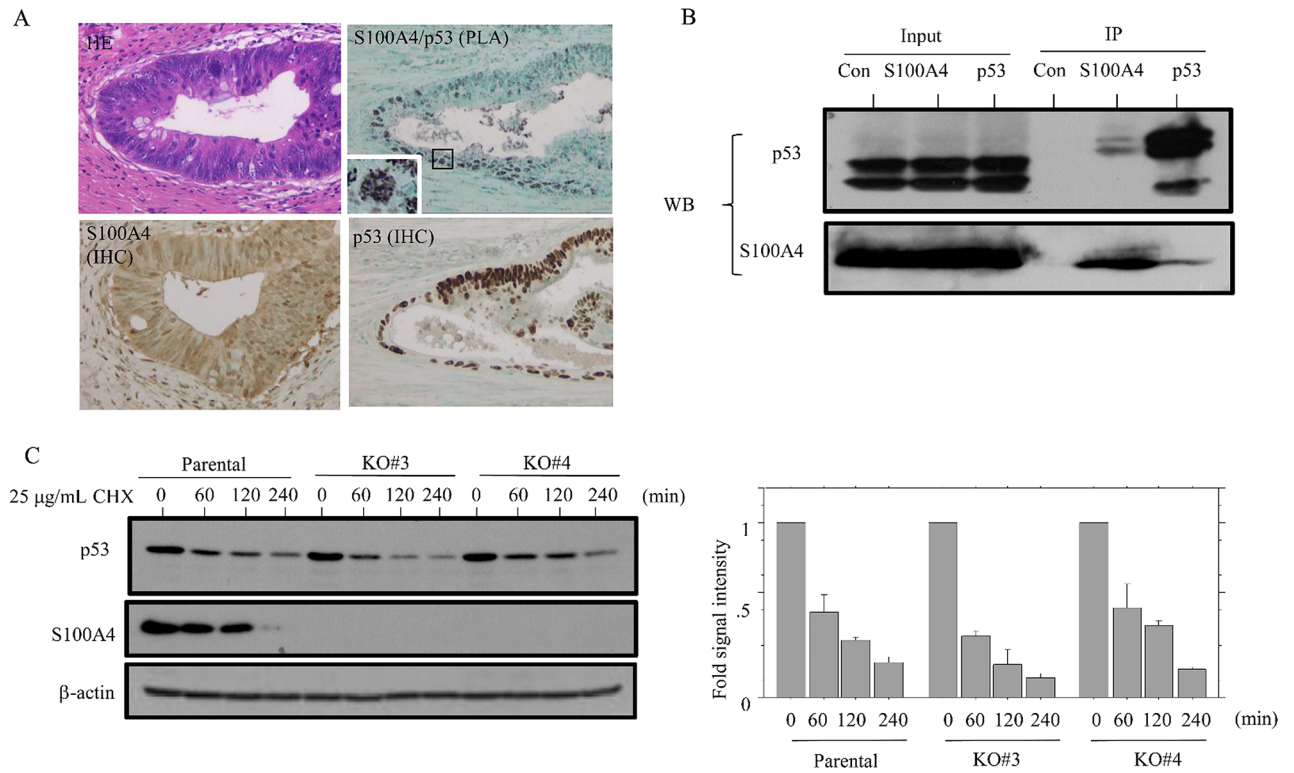


Fig. 5. Interaction between S100A4 and p53 in CRC cells. **(A)** PLA assay for the S100A4/p53 interaction, as well as IHC for S100A4 and p53, in NCRT-treated LAd-RC. Note the small aggregated dots in nuclear/cytoplasmic compartments of the tumor cells. Closed box in the PLA panel is magnified in the inset. Original magnification, x200 and x400 (inset). **(B)** After immunoprecipitation (IP) with the indicated antibodies using HCT116 cell lysates, western blot assay (WB) with anti-p53 (upper panel) and anti-S100A4 antibodies (lower panel) was carried out. Input was 5% of the total cell extract. Normal rabbit IgG was used as a negative control. The experiments were performed in triplicate. **(C)** Left: western blot analysis showing the indicated protein levels in S100A4 KO and parental cells treated with 25 µg/mL cycloheximide (CHX) at the indicated timepoints. Right: the ratios of p53 relative to β-actin were calculated using ImageJ version 1.41. The experiments were performed in duplicate.

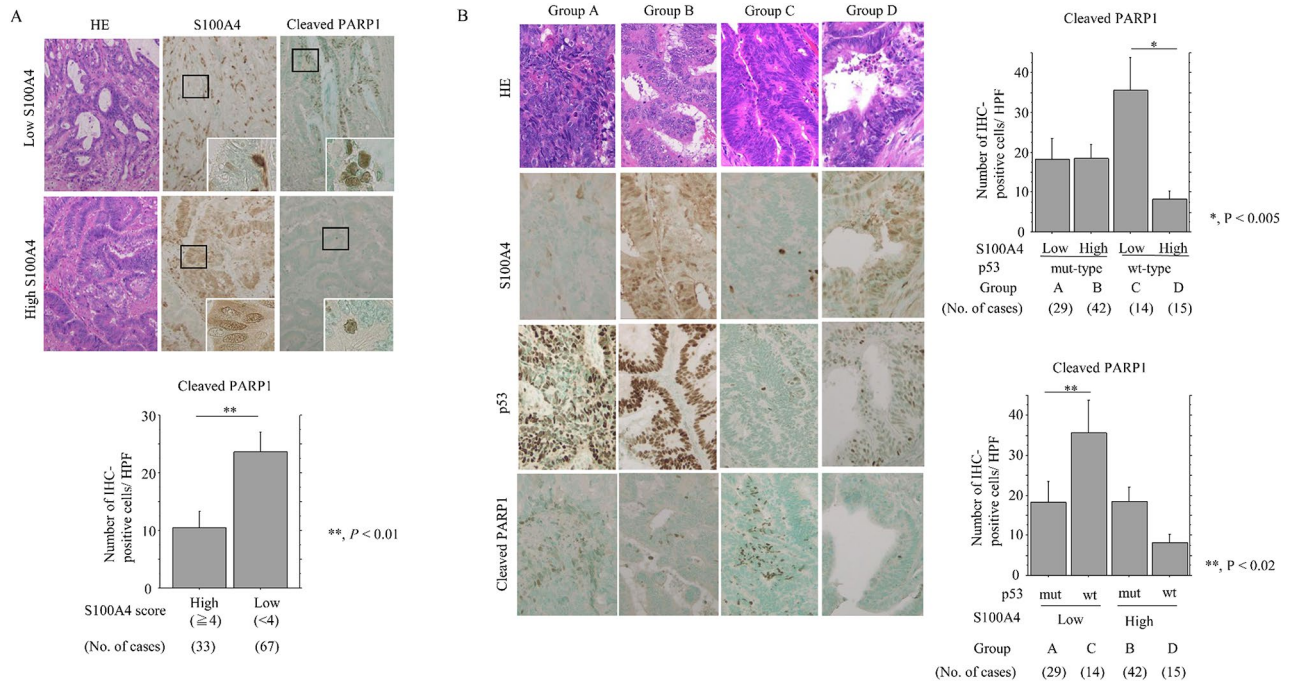


Fig. 6. Relationship between S100A4, p53 expression, and apoptosis in response to NCRT in LAd-RC. (A) Upper: staining with HE and IHC for the indicated proteins in samples of NCRT-treated LAd-RC cases with low (upper) and high (lower) S100A4 expression. The closed boxes in IHC panels are magnified in the insets. Original magnification, x100 and x400 (insets). Lower: number of cleaved PARP1-positive cells per high-power field (HPF) in S100A4-high and -low score categories in NCRT-treated LAd-RC. The number of positive cells is shown as mean ± SD. Statistical analyses were carried out using the Mann-Whitney U-test. (B) Left: staining with HE and IHC for the indicated proteins in samples of NCRT-treated LAd-RC cases. Original magnification, x200. Upper- and lower-right: number of cleaved PARP1-positive cells per high-power field (HPF) in cells with combined S100A4 and p53 status (a combination of high and low scores) in NCRT-treated LAd-RC. The number of positive cells is shown as mean ± SD. Statistical analyses were carried out using the Mann-Whitney U-test.

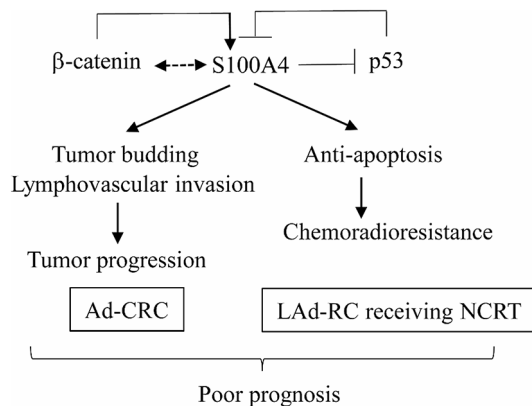


Fig. 7. Schematic representation of the interplay between S100A4, p53, and β-catenin in Ad-CRC and NCRT-treated LAd-RC. S100A4 expression acts as a poor prognostic factor through stimulation of tumor budding/lymphovascular invasion in Ad-CRC, and mediates chemoradioresistance due to its anti-apoptotic effects in NCRT-treated LAd-RC. This may occur through direct interactions with p53 and via indirect or direct interactions with nuclear β-catenin.

Data availability

The data sets generated during and/or analyzed during the current study are available from the corresponding author on reasonable request.

Received: 6 August 2024; Accepted: 9 December 2024

Published online: 28 December 2024

References

- Onyoh, E. F. et al. The rise of colorectal cancer in Asia: epidemiology, screening, and management. *Curr. Gastroenterol. Rep.* ; (2019). 21;36.
- Jasperson, K. W., Tuohy, T. M., Neklasen, D. W. & Burt, R. W. Hereditary and familial colon cancer. *Gastroenterology* ; (2010). 138;2044–58.
- Migliore, L., Migheli, E., Spisni, R. & Coppede, E. Genetics, cytogenetics, and epigenetics of colorectal cancer. *J Biomed Biotechnol.* ;2011;792362. (2011).
- Wong, M. C. et al. Prevalence and risk factors of colorectal cancer in Asia. *Intest Res.* ; (2019). 17;317–29.
- O'Connell, J. B., Maggard, M. A. & Ko, C. Y. Colon cancer survival rates with the new American joint committee on cancer sixth edition staging. *J. Nat. Cancer Inst.* ; (2004). 96;1420–5.
- Medich, D. et al. Preoperative chemoradiotherapy and radical surgery for locally advanced distal rectal adenocarcinoma: pathologic findings and clinical implications. *Dis. Colon Rectum.* **44**, 1123–1128 (2001).
- Ruo, L. et al. Long-term prognostic significance of extent of rectal cancer response to preoperative radiation and chemotherapy. *Ann. Surg.* **236**, 75–81 (2002).
- Sauer, R. et al. Preoperative versus postoperative chemoradiotherapy for rectal cancer. *N Engl. J. Med.* **351**, 1731–1740 (2004).
- Valentini, V. et al. Dose downstaging predict improved outcome after preoperative chemoradiation for extraperitoneal locally advanced rectal cancer? A long-term analysis of 165 patients. *Int. J. Radiat. Oncol. Biol. Phys.* ; (2002). 53;664–74.
- Reerink, O. et al. Molecular prognosis factors in locally irresectable rectal cancer treated preoperatively by chemo-radiotherapy. *Anticancer Res.* **24**, 1217–1221 (2004).
- Helfman, D. M., Kim, E. J., Lukanidin, E. & Grigorian, M. The metastasis associated protein S100A4: role in tumor progression and metastasis. *Br. J. Cancer* ; (2005). 92;1955–8.
- Garrett, S. C., Varney, K. M., Weber, D. J. & Bresnick, A. R. S100A4, a mediator of metastasis. *J. Biol. Chem.* ; (2006). 281;677–80.
- Bresnick, A. R., Weber, D. J. & Zimmer, D. B. S100 proteins in cancer. *Nat. Rev. Cancer.* **15**, 96–109 (2015).
- Mencia, N. et al. Overexpression of S100A4 in human cancer cell lines resistant to methotrexate. *BMC Cancer.* **10**, 250 (2010).
- Qi, R., Qiao, T. & Zhuang, X. Small interfering RNA targeting S100A4 sensitizes non-small-cell lung cancer cells (A549) to radiation treatment. *Onco Targets Ther.* **9**, 3753–3762 (2016).
- Dahlmann, M. et al. Combination of Wnt/b-catenin targets S100A4 and DKK1 improves prognosis of human colorectal cancer. *Cancers* ; (2022). 14;37.
- Japanese Society for Cancer of the Colon and Rectum. ed. General Rules for Clinical and Pathological Studies on Cancer of the Colon, Rectum and Anus, 3rd English edition. Tokyo, Japan: Japanese Classification of Colorectal, Appendiceal, and Anal Carcinoma, (2019).
- Brierley, J. D. et al. (eds) *TNM Classification of Malignant Tumours* (Wiley-Blackwell, 2016).
- Sato, T. et al. A multicenter phase I study of preoperative chemoradiotherapy with S-1 and irinotecan for locally advanced lower rectal cancer (SAMRAI-1). *Radiother Oncol.* **120**, 222–227 (2016).
- Zengin, M. & Cifci, A. Tumour budding in preoperative biopsy specimens is a useful prognostic index for identifying high-risk patients in early-stage (pN0) colon cancer. *Turk. J. Med. Sci.* **50**, 375–385 (2020).
- Ishibashi, Y. et al. Nucleobindin 2 inhibits senescence in gastric cancer. *Sci. Rep.* **14**, 11261 (2024).
- Yemelyanova, A. et al. Immunohistochemical staining patterns of p53 can serve as a surrogate marker for TP53 mutations in ovarian carcinomas: an immunohistochemical and nucleotide sequencing analysis. *Mod. Pathol.* **24**, 1248–1253 (2011).
- Saegusa, M. et al. Upregulation of TCF4 expression as a transcriptional target of b-catenin/p300 complexes during trans-differentiation of endometrial carcinoma cells. *Lab. Invest.* **85**, 768–779 (2005).
- Tochimoto, M. et al. S100A4/non-muscle myosin II signaling regulates epithelial-mesenchymal transition and stemness in uterine carcinosarcoma. *Lab. Invest.* **100**, 682–695 (2020).
- Itou, T. et al. EBP50 depletion and nuclear b-catenin accumulation engender aggressive behavior of colorectal carcinoma through induction of tumor budding. *Cancers* **16**, 183 (2024).
- Nakagawa, M. et al. Interaction between membranous EBP50 and myosin 9 as a favorable prognostic factor in ovarian clear cell carcinoma. *Mol. Oncol.* **17**, 2168–2182 (2023).
- Akiya, M. et al. Identification of LEFTY as a molecular marker for ovarian clear cell carcinoma. *Oncotarget* **8**, 63646–63664 (2017).
- Fredriksson, S. et al. Protein detection using proximity-dependent DNA ligation assays. *Nat. Biotechnol.* ; (2002). 20;473–7.
- Kwak, J. M. et al. Expression of protein S100A4 is a predictor of recurrence in colorectal cancer. *World J. Gastroenterol.* **16**, 3897–3904 (2010).
- Orre, L. M. et al. S100A4 interacts with p53 in the nucleus and promotes p53 degradation. *Oncogene* **32**, 5531–5540 (2013).
- Grigorian, M. et al. Tumor suppressor p53 protein is a new target for the metastasis-associated Mts1/S100A4 protein. *J. Biol. Chem.* **276**, 22699–22708 (2001).
- Goto, K., Endo, H. & Fijiyoshi, T. Cloning of the sequences expressed abundantly in established cell lines: identification of a cDNA clone highly homologous to S-100, a calcium binding protein. *J. Biochem.* **103**, 48–53 (1988).
- Linzer, D. I. & Nathans, D. Growth-related changes in specific mRNAs of cultured mouse cells. *Proc. Natl. Acad. Sci. USA.* **80**, 4271–4275 (1983).
- Ebralidze, A. et al. Isolation and characterization of a gene specifically expressed in different metastatic cells and whose deduced gene product has a high degree of homology to a Ca²⁺-binding protein family. *Genes Dev.* **3**, 1086–1093 (1989).
- De Vouge, M. W. & Mukherjee, B. B. Transformation of normal rat kidney cells by v-K-ras enhances expression of transin 2 and an S-100-related calcium-binding protein. *Oncogene* **7**, 109–119 (1992).
- Takenaga, K., Nakamura, Y., Endo, H. & Sakiyama, S. Involvement of S100-related calcium-binding protein pEL98 (or mts1) in cell motility and tumor cell invasion. *Jpn J. Cancer Res.* **85**, 831–839 (1994).
- Ueno, H. et al. Tumour 'budding' as an index to estimate the potential of aggressiveness in rectal cancer. *Histopathology* **40**, 127–132 (2002).
- Shinto, E. et al. A novel classification of tumour budding in colorectal cancer based on the presence of cytoplasmic pseudo-fragments around budding foci. *Histopathology* **47**, 25–31 (2005).
- Bertram, J., Palfner, K., Hiddemann, W. & Kneba, M. Elevated expression of S100P, CAPL and MAGE 3 in doxorubicin-resistant cell lines: comparison of mRNA differential display reverse transcription-polymerase chain reaction and subtractive suppressive hybridization for the analysis of differential gene expression. *Anticancer Drugs.* **9**, 311–317 (1998).
- Boye, K. et al. Prognostic significance of S100A4 expression in stage II and III colorectal cancer: results from a population-based series and a randomized phase III study on adjuvant chemotherapy. *Cancer Med.* **5**, 1840–1849 (2016).
- Boulares, A. H. et al. Role of poly(ADP-ribose) polymerase (PARP) cleavage in apoptosis. *J. Biol. Chem.* **274**, 22932–22940 (1999).
- Mahon, P. C. et al. S100A4 contributes to the suppression of BNIP3 expression, chemoresistance, and inhibition of apoptosis in pancreatic cancer. *Cancer Res.* **67**, 6786–6795 (2007).
- Pedersen, K. B., Andersen, K., Fodstad, O. & Maelandsmo, G. M. Sensitization of interferon-gamma induced apoptosis in human osteosarcoma cells by extracellular S100A4. *BMC Cancer* ; (2004). 4;52.

Acknowledgements

None.

Author contributions

YH, SI, YK, HT, and MS carried out the majority of the experiments, analyzed the data, and wrote the manuscript. They were helped by YO, Miki H, AY, AS, NE, MH, MO, and CK. All authors reviewed and approved the final manuscript.

Funding

This study was supported by a grant from JSPS KAKENHI Grant Number 22K06967.

Declarations

Competing interests

The authors declare no competing interests.

Consent for publication

Not applicable.

Ethics approval

This study was conducted in accordance with the principles expressed in the Declaration of Helsinki 1964 and later versions. This study was approved by the Kitasato University Medical Ethics Committee (B19-155). This article does not contain any studies with animals performed by any of the authors.

Informed consent

was obtained from all subjects involved in the study.

Additional information

Supplementary Information The online version contains supplementary material available at <https://doi.org/10.1038/s41598-024-82814-9>.

Correspondence and requests for materials should be addressed to M.S.

Reprints and permissions information is available at www.nature.com/reprints.

Publisher's note Springer Nature remains neutral with regard to jurisdictional claims in published maps and institutional affiliations.

Open Access This article is licensed under a Creative Commons Attribution-NonCommercial-NoDerivatives 4.0 International License, which permits any non-commercial use, sharing, distribution and reproduction in any medium or format, as long as you give appropriate credit to the original author(s) and the source, provide a link to the Creative Commons licence, and indicate if you modified the licensed material. You do not have permission under this licence to share adapted material derived from this article or parts of it. The images or other third party material in this article are included in the article's Creative Commons licence, unless indicated otherwise in a credit line to the material. If material is not included in the article's Creative Commons licence and your intended use is not permitted by statutory regulation or exceeds the permitted use, you will need to obtain permission directly from the copyright holder. To view a copy of this licence, visit <http://creativecommons.org/licenses/by-nc-nd/4.0/>.

© The Author(s) 2024